Innov Biosyst Bioeng, 2025, vol. 9, no. 1, 26–44
doi: 10.20535/ibb.2025.9.1.315523

Original article

ANTIFUNGAL ACTIVITY AND CYTOTOXICITY OF IMIDAZOLE- AND MORPHOLINE-BASED LYSOSOMOTROPIC DETERGENTS

D. Hodyna[1*], V. Kovalishyn[1], Yu. Shulha[1], O. Trokhimenko[2], O. Aksenovska[1], S. Rogalsky[1], L. Metelytsia[1]

[1]V.P. Kukhar Institute of Bioorganic Chemistry and Petrochemistry of the National Academy of Sciences of Ukraine, Kyiv, Ukraine
[2]Shupyk National Healthcare University of Ukraine, Kyiv, Ukraine

*Corresponding author: dianahodyna@gmail.com

Received 18 November 2024; Accepted 6 February 2025

Background. The spread of infectious diseases caused by drug-resistant bacteria and fungi, especially nosocomial strains, is currently considered a serious medical problem. It is known that the fungus *Candida albicans* is the most common causative agent of candidal infection, including the severe type. The emergence and rapid formation of drug resistance, as a risk factor in the treatment of oncological diseases burdened by candidal infection, requires new therapeutic approaches, including the study of synthetic bioregulators with antifungal and anticancer efficacy.
Objective. To synthesize and to determine the antifungal activity and cytotoxicity of imidazole- and morpholine-based lysosomotropic detergents (LDs) comprising both dodecyl radicals and ester-functionalized long alkyl chains.
Methods. To develop the QSAR models by the OCHEM platform, machine learning methods such as Transformer Convolutional Neural Network (Trans-CNN), Transformer Convolutional Neural Fingerprint (Trans-CNF), and Random Forest (RF) were used. Imidazole- and morpholine-based lysosomotropic detergents comprising both dodecyl radicals and ester-functionalized long alkyl chains were synthesized and characterized by ^{1}H Nuclear Magnetic Resonance spectroscopy. The antifungal properties of studied compounds were estimated by the disc diffusion method against the *C. albicans* ATCC 10231, *C. albicans*, *C. glabrata* and *C. krusei* clinical isolates. The *in vitro* cytotoxic activity of LDs was evaluated by IC_{50} value against the throat cancer HEp-2 cell lines. AutoDock Vina software was used for the evaluation of the synthesis compounds as ligands of several antifungal targets.
Results. The identified and synthesized imidazole- and morpholine-based LDs showed high antifungal potential against all *Candida spp.*, specifically against the fluconazole-resistant *C. albicans*, *C. glabrata*, and *C. krusei* clinical isolates. Imidazole-based LD 1 (IM-C_{12}) and morpholine-based LD 4 (Mor-C_{12}) were the most active against tested fungal strains. Molecular docking results suggest that the antifungal mechanisms of the compounds may be related to the inhibition of fungal lanosterol 14α-demethylase. The cytotoxic results of the synthesized compounds against the HEp-2 cell line demonstrated that morpholine-based LDs are less cytotoxic compared to imidazole-based
Conclusions. It was found that LD IM-C_{12} (1) is the most promising cytostatic and antifungal agent based on the obtained results. LDs IM-CH_2COOC_{10} (2) and Mor-C_{12} (4), which, under conditions of chemical modification, including through the carbon chain, may also be interesting for developing potential anticancer agents.

Keywords: lysosomotropic detergents; 1-alkylimidazole; N-alkylmorpholine; anti-Candida activity; cytotoxicity; molecular docking; QSAR.

Introduction

Lysosomotropic detergents (LDs) are specific biologically active compounds based on long-chain amines of intermediate pK_a (5.5-7.6). The known LDs are N-dodecylmorpholine and 1-dodecylimidazole [1]. Being lipophilic, these oily compounds diffuse readily across cell membranes and enter lysosomes, which are intracellular organelles containing a large set of hydrolytic enzymes [2]. In the acidic environment within lysosomes (pH 4.5−5.0) [3] LDs become protonated and acquire detergent properties, accumulating in membrane-bound compartments of low pH [1, 4]. Thus, the concentration of surface-active detergent inside the lysosomes increases and becomes sufficient to disrupt lysosomal membranes, releasing their enzymes into the cytosol and ultimately killing the cell.

In contrast to other detergents that kill cells by interaction with the outer cell membrane, LDs primarily act from the lysosome [5, 6]. The cytotoxicity of LDs strongly depends on the hydrocarbon chain length and is maximum for compounds with dodecyl radical, while shorter chain homologs are much less active or inactive [1, 5]. The most studied LD 1-dodecylimidazole (IM-C_{12}) was found

to be cytotoxic to mammalian cells at low concentrations, and the cysteine proteases are the major cytotoxic enzymes released from lysosomes [6].

Due to the enhanced lysosomal function, cancer cells are often more susceptible to lysosomal membrane permeabilization. The use of LDs to destabilize the lysosomal membrane and induce lysosome-dependent cell death is considered a promising strategy in cancer therapy [7, 8]. The extracellular pH (pH_e) of tumor cells is slightly acidic in the range of 6.4–7.0, whereas the pH_e of normal tissues is in the range of 7.2–7.5 [9]. This difference can be used for selective inhibition of cancer cells by LDs. Indeed, IM-C_{12} exhibited pH_e-dependent cytotoxicity against murine mammary carcinoma cell line EMT-6 and human bladder carcinoma MGH U1 cells. Cell killing was dose-dependent and was 100-fold greater at pH_e 6.0 than at pH_e 7.0. [10]. It has been shown that certain cell lines, such as promyelocytic cell line HL60 are more sensitive to C_{12}-IM in the rapidly proliferating phase than in the stationary phase [11]. This lysosomotropic detergent was also found to inhibit DNA synthesis in human colon cancer cells HCT116 and RCA and human breast cancer cells MCF-7 [12]. The results of a recent study showed that IM-C_{12} exhibited cytotoxic activities on K562 leukemia and SK-N-DZ neuroblastoma cell lines. Furthermore, this compound inhibited a panel of molecular targets involved in leukemia and neuroblastoma tumorigenesis [13].

Overall, LDs demonstrated promising anti-tumor properties and may be used for the development of new anti-cancer drugs. An important feature of LDs is their broad-spectrum antifungal activity [1, 4]. Invasive candidiasis is a common and serious health-care-associated fungal infection in critically ill patients and refers to the bloodstream and deep-seated infections of the genus *Candida* [14]. Invasive candidiasis is one of the common causes of morbidity and mortality in patients with solid tumors [15–17]. The growing increase of fungal infections may be attributed to the multiple invasive procedures, prolonged antibiotic treatment, as well as the use of high-dose immunosuppressants [17]. *C. albicans* is reported as the most frequent isolate in such cases followed by *C. parapsilosis*, *C. tropicalis*, or *C. glabrata* [16]. Because fungi are eukaryotes and many potential targets for antifungal development are also conserved in humans, invasive fungal infections are difficult to treat. The common antifungal drugs currently available for the treatment of invasive infections are limited to only three classes (polyenes, azoles, and echinocandins) [18]. Amphotericin B is the best-known fungicidal drug of class polyene that inhibits fungal ergosterol [19, 20]. However, Amphotericin B interacts with cholesterol in human cell membranes, which is responsible for its toxicity and numerous side effects [20]. Currently, the azole antifungals are most commonly used for the treatment and prophylaxis of invasive candidiasis. The primary mechanism of action of azoles is the inhibition of 14α-lanosterol demethylase, an enzyme required for the synthesis of ergosterol in the fungal cell membrane [21, 22]. The clinically useful compounds include imidazoles (clotrimazole, miconazole, ketoconazole) and triazoles (fluconazole, itraconazole). Fluconazole is often the drug of choice for the treatment of most invasive *Candida* infections and is considered an efficient alternative to Amphotericin B. However, *in vitro* and *in vivo* studies clearly demonstrated the endocrine disrupting potential of azole fungicides [22, 23]. Moreover, *C. albicans* was found to have an arsenal of defense mechanisms to overcome inhibition by the azole antifungals [24]. Widespread use of fluconazole and itraconazole is considered the main reason for fungal resistance to azoles [21]. Echinocandins (micafungin, anidulafungin, caspofungin), the newest addition to the arsenal of antifungals, have a unique mechanism of action, inhibiting β-(1,3)-D-glucan synthase, an enzyme responsible for fungal cell wall construction [25]. The echinocandins display fungicidal activity against most *Candida spp.*, including fluconazole-resistant strains. These natural product-derived novel antifungal drugs have much fever toxic side effects compared to azoles and polyenes. However, the cardiac toxicity of certain echinocandin antifungals has been observed [26]. Although the resistance of most Candida species to echinocandin-class drugs remains relatively low, high-level resistance has been reported among *C. glabrata* [27, 28].

Recent studies reveal that antifungal drugs may be efficient in cancer therapy due to the overlapping targets or molecular pathways between fungal and cancer pathogenesis [29]. Fungi possess vacuoles which are targets for LDs, similar to lysosomes in mammalian cells. Indeed, the most fungal strains were found to be highly susceptible to 1-dodecylimidazole (IM-C_{12}) and N-dodecylmorpholine (Mor-C_{12}) which disrupted the vacuoles and prevented fungal growth [1]. IM-C_{12} is more active than ketoconazole and somewhat less active than Amphotericin B [1]. Thus, LDs seem very promising alternative antifungal drugs which may also be used in anticancer therapy. However, like in the case of cationic surfactants, the presence of hydro-

phobic aliphatic chains in the LDs structure causes high cytotoxicity and non-selectivity [5, 6, 13, 30]. This may be caused by the fast diffusion of these compounds across the hydrophobic regions of cell membranes, as well as more efficient solubilization of the lysosomal membranes when protonated inside the lysosomes [5, 6]. The introduction of polar functional groups into the hydrocarbon chains of cationic surfactants is a common approach to reduce their lipophilicity that may delay their penetration through the cell membrane [13, 31]. It is obvious that such an approach can also be implemented to prepare LDs with reduced toxicity. However, only several studies have been conducted to synthesize ester-functionalized LDs. Hughes *et al.* [32] reported the synthesis of pH sensitive surfactant N-dodecyl 2-imidazole-propionate (DIP). The ester linkage between imidazole and dodecyl tail was found to be metabolically labile. This "soft" LD has distinct advantages over other membrane-destabilizing agents and can be easily deactivated by cellular enzymes. It was designed to be inactive at extracellular or intra cytoplasmic pH 7.4 while becoming active at the pH 6.2 prevalent in early endosomes [32]. A series of long-chain 1-(acyloxyalkyl)imidazoles with approximate pK_a of 5.2, which contain cleavable ester groups in the hydrocarbon chains, were synthesized [33]. These lipids were significantly less toxic than IM-C_{12}, and were hydrolyzed in serum and cell homogenate. Overall, the potential of "soft" LDs to enhance endosome to cytosol transfer makes them very promising in nucleic acid (ODN and gene) therapy, the treatment of intracellular bacterial infections, as well as in the stimulation of MHC-1 immunity [32].

It is worth noting that ester-functionalized LDs have not yet been studied for antifungal activity. In this article, new imidazole- and morpholine-based lysosomotropic detergents comprising ester-functionalized long alkyl chains were synthesized and studied for antifungal activity, as well as cytotoxicity against the throat cancer HEp-2 cell lines.

Materials and Methods

Dataset. The 1341 chemical compounds used for Quantitative Structure-Activity Relationship (QSAR) modeling were taken from the ChEMBL database [34]. These compounds were carefully selected for their activity against *C. krusei*, which were measured as MIC (minimum inhibitory concentration) in μg/mL values. The data were uploaded to the OCHEM database for QSAR modeling, and their activity values have been transformed into log(1/MIC) format for better analysis [35]. The OCHEM website provides public access to the chemical structures corresponding to the compounds used for QSAR modeling and a complete list of publications [36].

Machine learning methods. During the development of QSAR models, we experimented with different methods and sets of descriptors available in OCHEM. Our most successful models were produced using the Transformer Convolutional Neural Network (Trans-CNN) [37], Transformer Convolutional Neural Fingerprint (Trans-CNF) [38] and Random Forest (RF) [39] techniques. The optimized parameter settings were used for each machine learning method offered by the OCHEM platform.

The Trans-CNN utilizes molecule information encoded in SMILES notation to create QSAR models. This method predicts a target value by averaging individual predictions for a group of non-standard SMILES belonging to a single molecule. The variance within the group can be used to gauge the confidence interval of the forecast, and the capability to canonicalize SMILES helps in determining the uncertainty of the forecasts [37].

The Trans-CNF is a variation of the Trans-CNN that utilizes a convolutional neural fingerprint instead of a convolutional neural network to process the latent representation of the neural network. This approach also incorporates augmentation techniques commonly used in computer vision, which have more recently been introduced in QSAR studies [38].

RF is a powerful machine-learning algorithm that consists of decision trees. Each tree is built using a random subset of the training data and a randomly selected subset of features [39]. The RF algorithm then makes predictions by taking a majority vote on the predictions of individual trees. This approach is particularly effective for high-dimensional data and large datasets due to its non-parametric nature and efficient operation. In this case, the forest size was set to 512 trees, and the number of features tested at each split was determined by a specific formula based on the number of input features.

Molecular descriptor calculations. In our research, we utilized a variety of software packages supported by OCHEM to compute a wide range of molecular descriptors. Specifically, we implemented E-state indices [40], AlogPS [41], and CDK2 [42] software to construct the RF model.

The electro-topological state (E-State) indices are a set of parameters used to describe a mole-

cule's key structural aspects. These indices take into consideration both the electronic and topological properties of the compounds. They are widely used in computational chemistry and drug design to characterize the molecular structure and predict various properties of chemical compounds [40].

The AlogPS program is a computational tool used to calculate the estimates of the lipophilicity (logP) and solubility in water (logS) of chemical compounds [41].

The Chemical Development Kit (CDK) employs computational methods to calculate a set of 256 molecular descriptors. These descriptors encompass topological, geometrical, constitutional, electronic, and hybrid features providing a detailed and multifaceted representation of the molecules under study [42].

Model validation. The performance of the QSAR models was assessed through a fivefold cross-validation method and external validation sets [43]. To guard against inaccurate model estimations resulting from overfitting due to variable selection, OCHEM conducts multiple repetitions of all stages involved in model development within each validation fold. This meticulous approach aims to ensure that the resulting models are trustworthy and capable of making accurate predictions. The quality of the final models was verified using the aforementioned test sets.

Statistical parameters. To evaluate the performance of the regression models, we employed several important evaluation metrics. These metrics included the root mean square error (RMSE), which quantifies the average deviation of the predicted values from the actual values; the mean absolute error (MAE), which measures the average absolute deviation between the predicted and actual values; the squared correlation coefficient, R^2, which is a statistical measure indicating how well the model fits the data; and the coefficient of determination, q^2, which quantifies the predictive power of the model [44]. These metrics play a crucial role in assessing the accuracy and reliability of regression models, providing valuable insights that can guide further improvements or adjustments to the models.

OCHEM offers a valuable feature for estimating the applicability domain of developed models and the accuracy of forecasts, which is essential for ensuring the reliability and relevance of the models [45]. The platform's manual provides in-depth information on the machine learning techniques utilized, the descriptors chosen, the statistical coefficients used, and the detailed validation procedures followed. This comprehensive documentation is beneficial for understanding and replicating the modeling process [46].

Chemistry. Following chemicals were used for the synthesis: chloroacetyl chloride (98%), 1-decanol, 1-dodecanol (98%), 1-chlorododecane, 1-bromododecane (97%), 1-methylimidazole, morpholine (for synthesis), imidazole (99%), sodium hydride (60% mineral oil dispersion), acetonitrile (99.8%), benzene, hexane, ethyl acetate (98%), potassium carbonate (99%), hydrochloric acid (37%) were purchased from Sigma-Aldrich.

The alkylating agents, 1-decyl chloroacetate and 1-dodecyl chloroacetate were synthesized by the method described in [13] (Scheme 1). Alkyl esters of chloroacetic acid were obtained as transparent liquids.

1-Dodecylimidazole (IM-C_{12}) was synthesized according to Scheme 2. Sodium hydride (3.5 g, 60% suspension in mineral oil) was washed with dry hexane on the filter and then suspended in 70 ml of acetonitrile. To the stirred mixture, imidazole (5 g, 0.07 mol) was added in small amounts. The reaction was carried out for 4 h at room temperature. Then 1-bromododecane (15.8 g, 0.06 mol) was added and the mixture was refluxed for 6 h. After cooling to room temperature, it was poured into water (200 ml). The top organic layer was extracted with methylene chloride (2×50 ml) and dried over sodium sulfate. The methylene chloride was distilled off, residual solvent was removed under vacuum at 50 °C. The product was obtained as a light yellow liquid.

The structure of the synthesized compound was confirmed by the nuclear magnetic resonance (NMR) technique. ^{1}H NMR spectrum was recorded in $CDCl_3$ on a Varian Gemini-2000 (400 MHz) spectrometer.

1-dodecyl-1-H-imidazole (IM-C_{12}, compound 1)

^{1}H NMR (400 MHz,$CDCl_3$): δ = 0.87 (t, J = 6.5 Hz, 3H, CH_3), 1.17-1.33 (m, 18H, $CH_3(CH_2)_9$), 1.75 (t, J = 7.0 Hz, 2H, NCH_2CH_2), 3.9 (t, J = 7.2 Hz, 2H, NCH_2), 6.88 (t, J = 1.3 Hz, 1H, C_4-H), 7.03 (d, J = 1.2 Hz, 1H, C_5-H), 7.44 (d, J = 1.2 Hz, 1H, C_2-H).

Ester-functionalized imidazole-based LDs were synthesized using a similar approach (Scheme 2). The mixture of sodium imidazole (0.07 mol) and corresponding alkyl chloroacetate (0.06 mol) in acetonitrile (70 ml) was refluxed for 6 h. After cooling to room temperature, it was poured into water (200 ml). The formed precipitate was filtered off and dried in a vacuum. Finally, it was purified by recrystallization from hexane.

Decyl 2-(1H-imidazol-1-yl)acetate (IM-CH_2COOC_{10}, compound 2)

Yield: 65% (12.1 g), white solid, mp 85 °C

^{1}H NMR (400 MHz,$CDCl_3$): δ = 0.86 (t, *J* = 6.7 Hz, 3H, CH_3), 1.18-1.36 (m, 14H, $CH_3(CH_2)_7$), 1.62 (q, *J* = 6.9 Hz, 2H, NCH_2CH_2), 4.16 (t, *J* = 6.7 Hz, 2H, $COOCH_2$), 4.69 (s, 2H, NCH_2), 6.95 (d, *J* = 1.3 Hz, 1H, C_4-H), 7.09 (s, 1H, C_5-H), 7.50 (s, 1H, C_2-H).

Dodecyl 2-(1H-imidazol-1-yl)acetate (IM-CH_2COOC_{12}, compound 3)

Yield: 72% (14.8 g), white solid, mp 94-95 °C

^{1}H NMR (400 MHz,$CDCl_3$): δ = 0.87 (t, *J* = 6.7 Hz, 3H, CH_3), 1.18-1.35 (m, 18H, $CH_3(CH_2)_9$), 1.63 (t, *J* = 6.9 Hz, 2H, NCH_2CH_2), 4.16 (t, *J* = 6.7 Hz, 2H, $COOCH_2$), 4.69 (s, 2H, NCH_2), 6.95 (d, *J* = 1.3 Hz, 1H, C_4-H), 7.10 (s, 1H, C_5-H), 7.51 (s, 1H, C_2-H).

Morpholine-based LDs were synthesized by the following method (Scheme 3). The mixture of morpholine (17.4 g, 0.1 mol) and 0.05 mol of corresponding alkylating agent (1-bromododecane, decyl chloroacetate or dodecylchloroacetate) in acetone (70 ml) was heated to reflux for 6 h. After cooling to room temperature, the solid residue of morpholine hydrobromide was filtered off, and the solvent was removed in a vacuum. The products were obtained as light yellow liquids.

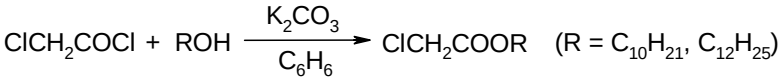

Scheme 1: Synthesis of long-chain alkyl chloroacetates

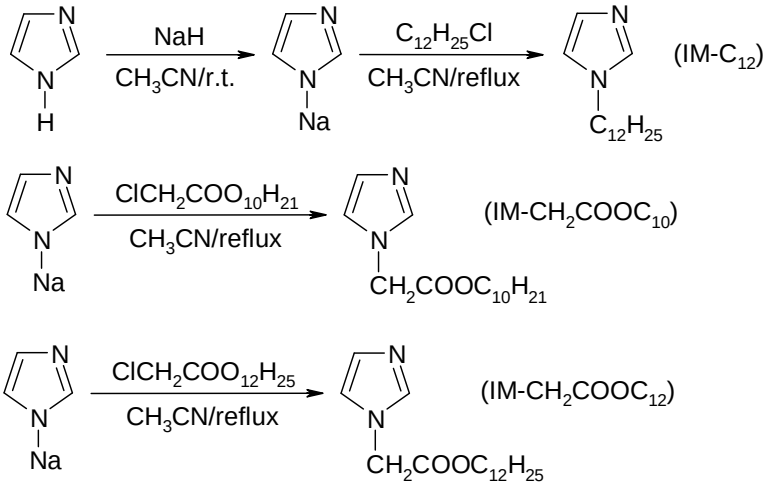

Scheme 2: Synthesis of imidazole-based lysosomotropic detergents

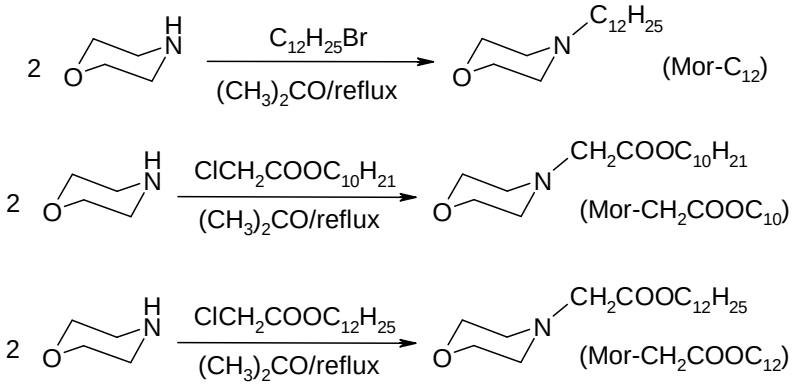

Scheme 3: Synthesis of morpholine-based lysosomotropic detergents

4-dodecylmorpholine (Mor-C_{12}, compound 4)

^{1}H NMR (400 MHz,$CDCl_3$): δ = 0.87 (t, *J* = 6.7 Hz, 3H, CH_3), 1.27 (m, 18H, $CH_3(CH_2)_9$), 1.47 (m, 2H, NCH_2CH_2), 2.33 (m, 2H, NCH_2), 2.43 (t, *J* = 4.6 Hz, 4H, CH_2-N-CH_2), 3.71 (m, 4H, CH_2-O-CH_2).

Decyl 2-morpholin-4-yl-acetate (Mor-CH_2COOC_{10}, compound 5)

Yield: 56% (8 g), yellow liquid

^{1}H NMR (400 MHz,$CDCl_3$): δ = 0.87 (t, *J* = 6.7 Hz, 3H, CH_3), 1.17-1.41 (m, 14H, $CH_3(CH_2)_7$), 1.63 (p, *J* = 6.9 Hz, 2H, $COOCH_2CH_2$), 2.51-2.65 (m, 4H, CH_2-N-CH_2), 3.21 (s, 2H, NCH_2), 3.69-3.82 (m, 4H, CH_2-O-CH_2), 4.12 (t, *J* = 6.8 Hz, 2H, $COOCH_2$).

Dodecyl 2-morpholin-4-yl-acetate (Mor-CH_2COOC_{12}, compound 6)

Yield: 64% (10 g), yellow liquid

^{1}H NMR (400 MHz,$CDCl_3$): δ = 0.88 (t, *J* = 6.7 Hz, 3H, CH_3), 1.18-1.40 (m, 18H, $CH_3(CH_2)_9$), 1.62 (q, *J* = 7.1 Hz, 2H, $COOCH_2CH_2$), 2.53-2.64 (m, 4H, CH_2-N-CH_2), 3.2 (s, 2H, NCH_2), 3.7-3.81 (m, 4H, CH_2-O-CH_2), 4.12 (t, *J* = 6.8 Hz, 2H, $COOCH_2$).

Antifungal activity evaluation. The antifungal properties of studied compounds were estimated by the disc diffusion method [47] against the *C. albicans* ATCC 10231, *C. albicans, C. glabrata* and *C. krusei* clinical isolates received from the Museum of Microbial Culture Collection of the Shupyk National Healthcare University of Ukraine. The inoculum concentration was 1×10^5 colony-forming units (CFU) per mL established using a 0.5 McFarland turbidity standard. 0.02 mL of tested compounds (10 mg/ml in dimethyl sulphoxide (DMSO)) was applied on standard paper disks (6 mm) which were placed on the Sabouraud agar plate. The plates were incubated at 37 °C for 24 h for antifungal activity. The compound content on a disc was 1.0 μmol, the fluconazole content on a disc was 0.03 μmol. The antifungal activity of the tested compounds was identified by measuring the zone diameter of growth inhibition. The compounds that formed zones of fungal growth inhibition < 8 mm were considered inactive. The experiments were done in triplicates. The results were expressed as mean ± SEM (standard error of the mean). Statistical analysis of the data was carried out using Student's t-test.

Cytotoxic activity evaluation. The *in vitro* cytotoxic activity of studied compounds was evaluated against the throat cancer HEp-2 cell lines. The cells were cultivated in RPMI-1640 medium (Sigma, USA) supplemented with cow embryos serum (5%) and antibiotics at 37 °C for 72 h in polystyrene 96-well culture plates (Sarstedt, Germany). A 100 μL of cell suspension with a cell density of 5×10^5 cells/mL was introduced into wells of culture plates and cultured at 37 °C in an atmosphere of 5% CO_2 for 24 h until complete formation of the cell monolayer. The compounds were dissolved in 1.5% DMSO to the final concentration of 2000 μg/mL, and serial two-fold and ten-fold dilutions of the studied compounds were prepared. The 100 μL of compounds were brought into cultural plate holes with the cell culture. The compounds' cytotoxic effects were observed after 24, 48, and 72 h of incubation with the cell culture at 37 °C under 5% CO_2 using the inverted microscope and expressed as IC_{50} value (the amount of compound (μM) which causes cell degeneration in half of the test objects). The cellular degeneration was determined concerning to the control values (without the test compound). Cisplatin [48], known for its anticancer and cytotoxic effects on cancer cells, was used as a positive control. DMSO (1.5%) was used as a negative control.

Docking procedure. Using molecular docking calculations, imidazole- and morpholine-based LDs **1**–**6** were evaluated as potential inhibitors of antifungal enzymes. Compounds were docked into active sites of lanosterol 14α-demethylase (LDM), exo-β-(1,3)-glucanase (Exg), 12-kDa FK506-binding protein (FKBP12), aspartyl proteinase 3 (Sap 3), aspartyl proteinase 5 (Sap 5), and thymidylate kinase (TMPK). The corresponding crystal structures of enzymes from *C. albicans* (PDB codes are 5TZ1 [49], 4M80 [50], 5HW7 [51], 2H6T [52], 2QZX [53], 5UIV [54]) were downloaded from Protein Data Bank (www.rcsb.org) [55]. Before docking calculation, the ligands and water molecules as well as unused subunits of enzymes were removed from downloaded files. The structures of imidazole- and morpholine-based LDs were drawn by Marvin Sketch software [56] and optimized using MMFF94s force field in the Avogadro program [57]. The ligands and enzymes pdbqt files were prepared using the program AutoDock Tools version 1.5.6 [58]. Molecular docking was performed by Autodock Vina software [59]. The grid centers for enzymes from *C. albicans* were 70.486, 65.238, 4.453 (LDM); 13.969, 38.141, 29.748 (Exg); 11.667, 85.721, 36.164 (FKBP12); 3.222, 5.556, 3.667 (Sap3); 20.382, 26.366, 41.534 (Sap5); 25.177, 14.322, 8.345 (TMPK).

Results

To form the external validation set, the initial data set of 1341 compounds was randomly divided into a training set of 1073 compounds (approximately 80% of the initial set) and a test set containing 268 compounds (20% of the initial set). The best QSAR models were generated using the Trans-CNN, Trans-CNF and RF methods (Fig. 1 and Table S1 in the *Supplementary materials*). The RF model was built with 339 descriptors, and 512 distinct trees were produced from randomly chosen subsets of these descriptors. The ultimate model was formed by aggregating the outcomes of individual trees through a majority vote (Fig. S1,c in the *Supplementary materials*). The q^2 values for the training and test sets fell within the ranges of 0.72−0.75 and 0.72−0.74, respectively. Further details regarding the statistical parameters of the models are available in Fig. 1. To quantitatively assess potential antifungal agents, a consensus model, formed by averaging three models, was utilized. The predictions derived from the consensus model were then employed to ascertain the model's applicability domain.

A virtual dataset of six drug-like imidazole- and morpholine-based LDs was created (*Supplementary Materials*, Table S1) and screened against *C. albicans* in the first stage using the previously published classification models [60]. Compounds **1**−**5** were identified as active within the applicability domain (Table 1). Then all compounds were screened against *C. krusei* using the developed consensus regression model. The four compounds (**2**, **4**, **5**, and **6**) predicted to be most active within the applicability domain (i.e., compounds with MICs < 50 μM; MICs were taken with the allowance for deviation) were selected for further evaluation (Table 1). Thus, all six compounds were selected for synthesis and biological testing (Table 2).

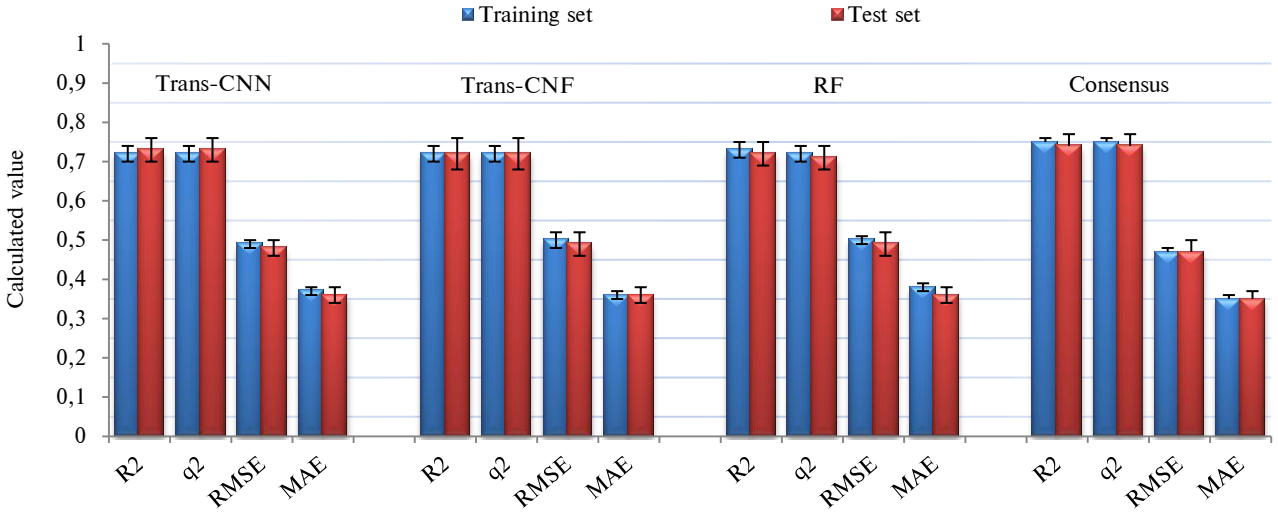

Figure 1: Parameters of the regression models. R^2 and q^2 are the squared linear correlation and coefficient of determination, respectively. RMSE is the root mean square error. MAE is the mean absolute error

Table 1: Evaluation activity of 6 compounds using consensus model developed against *C. krusei* and *C. albicans*

Comp.	*Candida albicans*				*Candida krusei*		
	M1	M2	Estimated accuracy	AD	log(1/MIC), mol/L	CONSENSUS-STD	AD
1	Active	Active	0.96	TRUE	4.18	0.47	FALSE
2	Active	Active	0.93	TRUE	3.96	0.35	TRUE
3	Active	Active	0.87	TRUE	4.06	0.34	FALSE
4	Active	Active	0.80	TRUE	4.56	0.17	TRUE
5	Active	Active	0.68	TRUE	4.36	0.12	TRUE
6	Active	Active	0.59	FALSE	4.42	0.09	TRUE

Notes. M1 – QSAR model developed by the ASNN (Associative Neural Network); M2 – QSAR model created by the WEKA-RF (Random Forest); MIC – minimum inhibitory concentration, mol/L; CONSENSUS-STD – the standard deviation of the predictions, obtained from an ensemble of models; AD – applicability domain.

The results presented in Table 2, demonstrated that all tested compounds with predicted high activity showed good antifungal potential against all *Candida spp.* strains. It should be noted that imidazole-based LD **1** (IM-C_{12}) and morpholine-based LD **4** (Mor-C_{12}) were highly active against *C. albicans* ATCC 10231 strain and *C. albicans*, *C. glabrata* and *C. krusei* clinical isolates with growth inhibition zones in the range of 31.3–37.3 mm and 30.3–39.7 mm respectively. Compounds **2, 3, 5** and **6** with ester-functionalized long alkyl chains $COOC_{10}$-$COOC_{12}$ demonstrated moderate effects against tested fungi with an inhibition zone of 9.0–22.3 mm. In addition, the studied compounds showed good activity specifically against the fluconazole-resistance *C. albicans*, *C. glabrata*, and *C. krusei* clinical isolates (growth inhibition zones from 13.0 to 39.7 mm).

The results presented in Table 3 show that the cytotoxic effect of the imidazole-based LDs **1**, **2**, and **3** has a pronounced cumulative character and differs only in the level of action (4.24 ± 0.28, 132.93 ± 12.96, and 231.29 ± 15.43 respectively). In general, during the first 24 h of observation, the level of cytotoxic activity can be recorded as IM-C_{12} > IM-CH_2COOC_{10} > IM-CH_2COOC_{12}. After 48–72 h of observation, all investigated imidazole-based LDs show a significant increase in cytotoxicity by 400, 3 and 2 times, respectively, maintaining the previously indicated trend of cytostatic effect – IM-C_{12} > IM-CH_2COOC_{10} > IM-CH_2COOC_{12}.

The cytotoxic results of the morpholine-based LDs showed that only Mor-C_{12} (**4**) has a cumulative cytotoxic effect with an IC_{50} of 82.27 ± 4.19 μM after 24 h of observation and a further 2-fold increase after 48–72 h. Morpholine-based LDs **5** and **6** with an IC_{50} of 261.98 ± 17.27 μM and 79.74 ± 5.56 μM had no cumulative effect throughout the observation period from 24 to 72 h. It should be noted that the presence of a cumulative cytotoxic effect is an important characteristic of cytostatic, which determines both their further study and the prospects of their use, taking into account the terms of the potential effect.

As for the cytostatic cisplatin, used in the study as a known antitumor agent, it should be noted that this drug does not have a cumulative effect, but the level of its cytotoxic effect (IC_{50} = 39.77 ± 1.10) is similar to the cytotoxic potential of IM-CH_2COOC_{10} (**2**) and Mor-C_{12} (**4**) with an IC_{50} of 39.51 ± 3.07 and 38.33 ± 3.67, respectively, after 48–72 h of exposure.

Table 2: Anti-Candida activity of studied compounds by diameters of inhibition zones

Compound		Content on a disc, μmol	Zone of inhibition, mm			
			C. albicans ATCC 10231	*C. albicans* isolate	*C. glabrata* isolate	*C. krusei* isolate
1	IM-C_{12}	1.0	31.3 ± 0.9	30.3 ± 0.9	33.3 ± 1.2	37.3 ± 1.2
2	IM-CH_2COOC_{10}	1.0	12.7 ± 0.3	17.3 ± 0.9	20.0 ± 0.6	22.3 ± 0.9
3	IM-CH_2COOC_{12}	1.0	9.7 ± 0.3	14.7 ± 0.3	13.0 ± 0.6	15.0 ± 0.6
4	Mor-C_{12}	1.0	35.3 ± 0.9	30.3 ± 1.2	39.7 ± 0.3	38.3 ± 1.5
5	Mor-CH_2COOC_{10}	1.0	11.0 ± 0.6	16.0 ± 0.6	17.7 ± 0.3	15.0 ± 0.6
6	Mor-CH_2COOC_{12}	1.0	9.0 ± 0.6	19.3 ± 0.9	20.3 ± 0.9	13.7 ± 0.3
Fluconazole		0.03	21.3 ± 0.9	n/a*	n/a	n/a

Notes. *n/a – no activity (growth inhibition zones < 8 mm). Values are expressed as mean ± SEM of the three replicates.

Table 3: Cytotoxicity of studied compounds against the HEp-2 cell line

Compound		IC_{50} (μM)		
		24 h	48 h	72 h
1	IM-C_{12}	4.24 ± 0.28	<0.01	<0.01
2	IM-CH_2COOC_{10}	132.93 ± 12.96	39.51 ± 3.07	39.51 ± 3.07
3	IM-CH_2COOC_{12}	231.29 ± 15.43	127.04 ±12.42	127.04 ± 12.42
4	MorC_{12}	82.27 ± 4.19	38.33 ± 3.67	38.33 ± 3.67
5	Mor-CH_2COOC_{10}	261.98 ± 17.27	261.98 ± 17.27	261.98 ± 17.27
6	Mor-CH_2COOC_{12}	79.74 ± 5.56	79.74 ± 5.56	79.74 ± 5.56
Cisplatin		39.77 ± 1.10	39.77 ± 1.10	39.77 ± 1.10

While the anticancer mechanisms of imidazole- and morpholine-based LDs **1**–**6** can been associated with specific binding to the DNA [61], SIRT1 deacetylase and Aurora kinase A [13], the antifungal mechanisms were evaluated by a molecular docking approach considering the compounds as possible ligands of fungal enzymes, which are important for the development and growth of microorganisms. Lanosterol 14α-demethylase (LDM), exo-β-(1,3)-glucanase (Exg), 12-kDa FK506-binding protein (FKBP12), aspartyl proteinase 3 (Sap 3), aspartyl proteinase 5 (Sap 5), and thymidylate kinase (TMPK) were considered as potential targets of the compounds. It is known that LDM is the target for azole antifungals, which are widely used in medicine and agriculture [62]. Exg is important for the development, differentiation, and defense of fungal cells [63]. FKBP12 belongs to of peptidyl-prolyl isomerase superfamily, which catalyzes the cis/trans isomerization of N-terminal peptide bonds to proline residues in polypeptide chains, plays an essential role in cell protein homeostasis [64]. Sap 3 and Sap 5 are important virulence factors of *C. albicans*. TMPK is a key enzyme in the yeast pyrimidine synthesis pathway [65].

The results of molecular docking studies (Table 4) indicate that the antifungal mechanism of imidazole- and morpholine-based LDs **1**–**6** can be explained through possible inhibition of LDM. A comparison of the docking energies obtained for LDM showed that morpholine-based LDs **4**–**6** have better results than imidazole-based LDs **1**–**3**. These can be explained by additional hydrogen bonds which can be formed between morpholine fragments of the compound and amino acid residues of the enzyme. Lengthening of the alkyl chain in the structure of the inhibitor optimizes the binding energy of the enzyme-inhibitor complex.

The binding mode of morpholine-based LD **6** in the active site of LDM from *C. albicans* is shown in Fig. 2. The complex stabilization occurs due to the hydrogen bonds of the morpholine ring with the amino acid residue His377 and the carbonyl group with the amino acids Tyr118 and Phe380.

Table 4: Docking energies (kcal/mol) of imidazole- and morpholine-based LDs at active sites of enzymes from *C. albicans*

Compound	*LDM*	*Exg*	*FKBP12*	*Sap3*	*Sap5*	TMPK
1	–6.3	–3.7	–4.7	–3.2	–5.0	–4.3
2	–6.6	–3.6	–5.2	–2.7	–5.1	–4.0
3	–6.8	–4.1	–5.4	–2.7	–5.4	–4.8
4	–6.9	–4.3	–5.0	–2.3	–5.0	–4.3
5	–7.0	–5.2	–5.4	–3.1	–4.2	–4.6
6	–7.5	–3.6	–4.9	–3.0	–5.4	–4.5

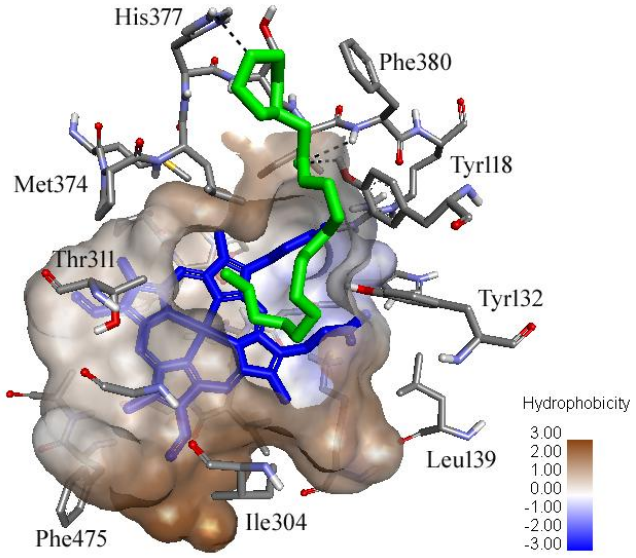

Figure 2: Possible binding modes of morpholine-based LD **6** at the active site of LDM

Discussion

It is known that one of the current research areas in the field of development of new biologically active compounds, including pharmaceutical products, is the search and analysis of new compounds that have a dual type of activity [66]. A number of authors presented 2-methoxydiol derivatives as new tubulin and HDAC dual-targeting inhibitors, displaying antitumor and antiangiogenic response [67], 2-aminopyrimidine derivatives as an immunosuppressive or antiinflammatory agent, dihydropyrazole-carbohydrazide derivatives with dual activity as antioxidant and anti-proliferative drugs [68], 2-(4-methylsulfonyl phenyl) indole derivatives with dual antimicrobial and anti-inflammatory activities [69] and other.

Based on data from the literature on the biological potential of imidazole- and morpholine-based derivatives, we conducted research aimed at *in silico* and *in vitro* evaluation of compounds of this class as promising prodrugs with a dual type of pharmacological action. The calculation methods of QSAR prediction used in the work made it possible to identify several compounds with potentially high activity, synthesize them, and *in vitro* evaluate their properties corresponding to the research objectives.

The fungal plasma membrane acts as a permeability barrier, as well as a matrix for proteins. It consists of sterols, phospholipids, and sphingolipids that determines the membrane's fluidity. Since fungal sterols are not present in mammalian cells, they are attractive therapeutic targets [70]. Imidazole derivatives are known to possess various pharmacological properties and are widely implicated in biochemical processes. Thus, imidazoles inhibit the cytochrome P450 dependent 14α-demethylation step in the formation of ergosterol which is the main sterol of fungal cell membranes. This inhibition causes accumulation of 14α methyl sterols in the membranes of fungi resulting in altered cell membrane properties. The results of *in vitro* studies with various strains of *C. albicans* showed direct correlation between the ability of imidazole-based drugs to inhibit sterol biosynthesis and their influence on fungal growth [70, 71]. It is worth noting that 1-alkyl-3-methylimidazolium salts, comprising long alkyl chains in the cation structure, have also been found to possess broad-spectrum antifungal activity [72–74]. Similar to common imidazole derivatives, cell membrane has been identified as the potential target in the case of imidazolium salts. Moreover, these compounds were also found to inhibit fungal ergosterol biosynthesis [74]. As for morpholine derivatives, they seem even more promising antifungals as they act on two different enzymes of ergosterol biosynthesis pathway: sterol Δ^{14} reductase and sterol Δ^{7}-Δ^{8} isomerase, leading to accumulation of intermediates ignosterol and lichesterol [70]. Another N-substituted morpholine derivatives comprising hydrophobic substituents, such as Amarolfine, Aldimorph, Fenpropimorph, are widely used commercial antifungals [70].

The results of our study indicate the high antifungal activity of common lysosomotropic detergents IM-C_{12} and Mor-C_{12} that is in good agreement with literature data [1]. According to results of molecular docking studies, the binding energy of Mor-C_{12} in the active site of LDM enzyme is stronger compared to IM-C_{12}. This is probably due to the formation of additional hydrogen bonds between morpholine rings and the amino acid residue His377 and the carbonyl group with the amino acids Tyr118 and Phe380 (Fig. 2). The introduction of polar ester groups into the alkyl chains of both imidazole- and morpholine-based LDs (compounds **2**, **3**, **5**, **6**) significantly increases the binding energies of these compounds in the active site of LDM (Table 2). However, the results of *in vitro* studies indicate that ester-functionalized LDs have significantly reduced antifungal activity compared to common antifungals IM-C_{12} and Mor-C_{12} (Table 1). The presence of polar ester groups in the hydrophobic alkyl chains of LDs reduce their lipophilicity that may delay their penetration through the cell membrane [13]. Thus, ester-functionalized LDs, as well as cationic biocides are known to possess reduced antimicrobial activity, as well as significantly reduced cytotoxicity compared to common long-chain analogues [13, 32, 33]. Ester-functionalized LDs are less protonated inside the lysosomes due to their lowered basicity [13, 33]. This also may lead to reduced cytotoxicity due to the lower concentration of cationic surfactants, which are able to break up the lysosomal membrane. The results of cytotoxicity studies against the HEp-2 cell line revealed much higher IC_{50} values for ester-functionalized imidazole derivatives (compounds **2** and **3**), as well as morphopline derivatives (compounds **5** and **6**) compared to IM-C_{12} and Mor-C_{12}, respectively (Table 3). Compounds **3** and **5** seem the most promising new antifungal agents since they combine moderate activity against studied fungal species, including clinical isolates, and low cytotoxicity. It should also be noted that the "soft" LDs, comprising cleavable ester groups in the alkyl chains, can be easily degraded by cellular enzymes

that is distinct advantage over other destabilizing membrane agents [32, 33]. However, further studies are needed to determine the spectrum of antifungal activity of these compounds, as well as their different levels of toxicity.

Conclusions

The developed QSAR consensus model of antifungal activity of imidazole- and morpholine-based LDs using the OCHEM web platform demonstrated robust predictive ability with a q^2 value of 0.75 ± 0.01. Moreover, the consensus prediction for the external evaluation set demonstrated high predictive power with a q^2 value of 0.74 ± 0.03. Using the model to screen a virtual chemical library for antifungal activity, six novel antifungal compounds were identified. The synthesized six imidazole- and morpholine-based LDs demonstrated good antifungal potential against all *Candida* strains including the fluconazole-resistant *C. albicans*, *C. glabrata*, and *C. krusei* clinical isolates. The most active were imidazole-based LD **1** (IM-C_{12}) and morpholine-based LD **4** (Mor-C_{12}) against the *C. albicans* ATCC 10231 and clinical isolates of *C. albicans*, *C. glabrata*, and *C. krusei* with growth inhibition zones in the range of 31.3–37.3 mm and 30.3–39.7 mm, respectively. The calculated results of molecular docking suggest that the antifungal mechanisms of the studied compounds may be associated with the inhibition of fungal lanosterol 14α-demethylase. The experimentally evaluated cytotoxic potential of the synthesized compounds showed that morpholine LDs are less cytotoxic than imidazole-based. Taking into account all the obtained experimental results of cytotoxic activity, imidazole-based LD **1** (IM-C_{12}) is the most promising cytostatic. Also worthy of attention are the compounds IM-CH_2COOC_{10} (**2**) and Mor-C_{12} (**4**), which, under conditions of chemical modification, including through the carbon chain, may also be of interest for the development of potential anticancer agents.

Interests disclosure

The authors declare no conflict of interest.

Funding

This work was supported by Grant of the NAS of Ukraine to research laboratories/groups of young scientists of the NAS of Ukraine to conduct research in the priority directions of the development of science and technology in 2024–2025 "Novel synthetic nitrogen-containing heterocyclic compounds with antimicrobial and anti-cancer activity" under Contract No. №29/02-2024(5) from 19.02.2024.

References

[1] Firestone RA, Pisano JM, Garrity GM, Fromtling RA, Zimmerman SB. Lysosomotropic agents. Broad-spectrum antifungal activity of lysosomotropic detergents. J Med Chem. 1987;30:1519-21. DOI: 10.1021/jm00391a043

[2] Hu M, Chen J, Liu S, Xu H. The acid gate in the lysosome. Autophagy. 2023;19:1368-70. DOI: 10.1080/15548627.2022.2125629

[3] Tancini B, Buratta S, Delo F, Sagini K, Chiaradia E, Pellegrino RM, et al. Lysosomal exocytosis: the extracellular role of an intracellular organelle. Membranes. 2020;10(12):406. DOI: 10.3390/membranes10120406

[4] Hussain M, Leibowitz MJ, Lenard J. Killing of Saccharomyces cereviciae by the lysosomotropic detergent N-dodecylimidazole. Antimicrob. Agents Chemother. 1987;31:512-17. DOI: 10.1128/AAC.31.4.512

[5] Miller DK, Griffiths E, Lenard J, Firestone RA. Cell killing by lysosomotropic detergents. J. Cell Biol. 1983;97:1841-51. DOI: 10.1083/jcb.97.6.1841

[6] Wilson PD, Firestone RA., Lenard J. The role of lysosomal enzymes in killing of mammalian cells by the lysosomotropic detergent N-dodecylimidazole. J. Cell Biol. 1987;104:1223-9. DOI: 10.1083/jcb.104.5.1223

[7] Eriksson I, Öllinger K. Lysosomes in cancer – at the crossroad of good and evil. Cells. 2024;13:459. DOI: 10.3390/cells13050459

[8] Trybus W, Trybus E, Król T. Lysosomes as a target in anticancer therapy. Int J Mol Sci. 2023;24:2176. DOI: 10.3390/ijms24032176

[9] Hao G, Xu ZP, Li L. Manipulating extracellular tumour pH: an effective target for cancer therapy. RSC Adv. 2018;8:22182-92. DOI: 10.1039/c8ra02095g

[10] Boyer MJ, Horn I, Firestone RA, Steele-Norwood D, Tannock IF. pH dependent cytotoxicity of N-dodecylimidazole: a compound that acquires detergent properties under acidic conditions. Br J Cancer. 1993;67:81-7. DOI: 10.1038/bjc.1993.13

[11] Wilson PD, Hreniuk D, Lenard J. Reduced cytotoxicity of the lysosomotropic detergent N-dodecylimidazole after differentiation of HL60 promyelocytes. Cancer Res. 1989;49:507-10.

[12] Dubowchik GM, Gawlak SL, Firestone RA. The *in vitro* effects of three lysosomotropic detergents against three human tumor cell lines. Bioorg Med Chem Lett. 1995;5:893-8. DOI: 10.1016/0960-894X(95)00136

[13] Gryniukova A, Borysko P, Myziuk I, Alieksieieva D, Hodyna D, Semenyuta I, et al. Anticancer activity features of imidazole-based ionic liquids and lysosomotropic detergents: in silico and in vitro studies. Mol Divers. 2024;28:3817-33. DOI: 10.1007/s11030-023-10779-4

[14] Pappas PG, Lionakis MS, Arendrup MS, Ostrovsky-Zeichner L, Kullberg BJ. Invasive candidiasis. Nat Rev Dis Primers. 2018;4:18026. DOI: 10.1038/nrdp.2018.26

[15] Ruijters VJ, Oosterom N, van der Perk M, Wolfs TFW, Meijer AJM, van den Heuvel-Eibrink MM, et al. Clinical characteristics of invasive fungal infections in pediatric oncology patients with solid tumors. J Pediatr Hematol Oncol. 2021;43(3):e408-13. DOI: 10.1097/MPH.0000000000001761

[16] De Rosa FG, Busca A, Capparella MR, Yan JL, Aram JA. Invasive candidiasis in patients with solid tumors treated with anidulafungin: a post hoc analysis of efficacy and safety of six pooled studies. Clin Drug Investig. 2021;41(6):539-48. DOI: 10.1007/s40261-021-01024-7

[17] Bai X, Luo J. Invasive candidiasis in patients with solid tumors: a single-center retrospective study. Int J Gen Med. 2023;16:2419-26. DOI: 10.2147/IJGM.S411006

[18] Pokharel M, Konarzewska P, Roberge JY, Han G-S, Wang Y, Carman GM, et al. The anticancer drug bleomycin shows potent antifungal activity by altering phospholipid biosynthesis. Microbiol Spectr. 2022;10:e0086222. DOI: 10.1128/spectrum.00862-22

[19] Hamill RJ. Amphotericin B formulations: a comparative review of efficacy and toxicity. Drugs. 2013;73(9):919-34. DOI: 10.1007/s40265-013-0069-4

[20] Dixon DM, Walsh TJ. Antifungal agents. In: Baron S, editor. Medical microbiology. 4th edition. Galveston (TX): University of Texas Medical Branch at Galveston; 1996. Chapter 76. Available from: https://www.ncbi.nlm.nih.gov/books/NBK8263/

[21] Kanafani ZA, Perfect JR. Resistance to antifungal agents: mechanism and clinical impact. Clin Infect Dis. 2008;46:120-8. DOI: 10.1086/524071

[22] Draskau MK, Svingen T. Azole fungicides and their endocrine disrupting properties: perspectives on sex hormone-dependent reproductive development. Front Toxicol. 2022;4:883254. DOI: 10.3389/ftox.2022.883254

[23] Munkboel CH, Rasmussen TB, Elgaard C, Olesen M-LK, Kretschmann AC, Styrishave B. The classic azole antifungal drugs are highly potent endocrine disruptors *in vitro* inhibiting steroidogenic CYP enzymes at concentrations lower than therapeutic Cmax. Toxicology. 2019;425:152247. DOI: 10.1016/j.tox.2019.152247

[24] Nishimoto AT, Sharma C, Rogers PD. Molecular and genetic basis of azole antifungal resistance in the opportunistic pathogenic fungus *Candida albicans*. J Antimicrob Chemoter. 2020;75(2):257-70. DOI: 10.1093/jac/dkz400

[25] Sucher AJ, Chahine EB, Balcer HE. Echinocandins: the newest class of antifungals. Ann Pharmacother. 2009;43:1647-57. DOI: 10.1345/aph.1M237

[26] Zhu P, Li Y, Guo T, Liu S, Tancer RJ, Hu C, et al. New antifungal strategies: drug combination and co-delivery. Adv Drug Deliv. Rev. 2023;198:114874. DOI: 10.1016/j.addr.2023.114874

[27] Perlin DS. Echinocandin resistance in Candida. Clin Infect Dis. 2015;61:S612-7. DOI: 10.1093/cid/civ791

[28] Pristov KE, Ghannoum MA. Resistance of *Candida* to azoles and echinocandins worldwide. CMI. 2019;25:792-8. DOI: 10.1016/j.cmi.2019.03.028

[29] Weng N, Zhang Z, Tan Y, Zhang X, Wei X, Zhu Q. Repurposing antifungal drugs in cancer therapy. J Adv Res. 2023;48:259-73. DOI: 10.1016/j.jare.2022.08.018

[30] Seo I, Jha BK, Lim JG, Suh SI, Suh MH, Baek WK. Identification of lysosomotropic compounds based on the distribution and size of lysosomes. Biochem Biophys Res Commun. 2014;450:189-94. DOI: 10.1016/j.bbrc.2014.05.091

[31] Trush M, Metelytsia L, Semenyuta I, Kalashnikova L, Papeykin O, Venger I, et al. Reduced ecotoxicity and improved biodegradability of cationic biocides based on ester-functionalized pyridinium ionic liquids. Environ Sci Poll Res. 2019;26:4878-89. DOI: 10.1007/s11356-018-3924-8

[32] Hughes JA, Aronsohn AI, Avrutskaya AV, Juliano RL. Evaluation of adjuvants that enhance the effectiveness of antisense oligodeoxynucleotides. Pharm Res. 1996;13:404-10. DOI: 10.1023/a:1016044609972

[33] Chen FJ, Asokan A, Cho MJ. Cytosolic delivery of macromolecules: I. Synthesis and characterization of pH-sensitive acyloxyalkylimidazoles. BBA. 2003;1611:140-50. DOI: 10.1016/s0005-2736(03)00049-x

[34] Mendez D, Gaulton A, Bento AP, Chambers J, De Veij M, Félix E, et al. ChEMBL: towards direct deposition of bioassay data. Nucleic Acids Res. 2019;47(D1):D930-40. DOI: 10.1093/nar/gky1075

[35] Sushko I, Novotarskyi S, Kцrner R, Pandey AK, Rupp M, Teetz W, et al. Online chemical modeling environment (OCHEM): web platform for data storage, model development and publishing of chemical information. J Comput Aided Mol Des. 2011;25(6):533-554. DOI: 10.1007/s10822-011-9440-2

[36] Online chemical databse with modeling environment [Internet]. Ochem.eu. 2025 [cited 2024 Sept 9]. Available from: https://ochem.eu/

[37] Karpov P, Godin G, Tetko IV. Transformer-CNN: Swiss knife for QSAR modeling and interpretation. J Cheminform. 2020;12(1):17. DOI: 10.1186/s13321-020-00423-w

[38] Tetko IV, Karpov P, Bruno E, Kimber TB, Godin G. Augmentation is what you need! In: Tetko I, Kůrková V, Karpov P, Theis F, editors. Artificial neural networks and machine learning – ICANN 2019: Workshop and special sessions. Lecture Notes in Computer Science, vol. 11731. Cham: Springer; 2019. DOI: 10.1007/978-3-030-30493-5_79

[39] Breiman L. Random forests. Mach Learn. 2001;45:5-32. DOI: 10.1023/A:1010933404324

[40] Hall LH, Kier LB. Electrotopological state indexes for atom types: A novel combination of electronic, topological, and valence state information. J Chem Inf Comput Sci. 1995;35:1039-45. DOI: 10.1021/ci00028a014

[41] Tetko IV, Tanchuk VY. Application of associative neural networks for prediction of lipophilicity in ALOGPS 2.1 program. J Chem Inf Comput Sci. 2002;42(5):1136-45. DOI: 10.1021/ci025515j

[42] Willighagen EL, Mayfield JW, Alvarsson J, Berg A, Carlsson L, Jeliazkova N, et al. The Chemistry Development Kit (CDK) v2.0: atom typing, depiction, molecular formulas, and substructure searching. J Cheminform. 2017;9(1):33. DOI: 10.1186/s13321-017-0220-4

[43] Tetko IV, Sushko I, Pandey AK, Zhu H, Tropsha A, Papa E, et al. Critical assessment of QSAR models of environmental toxicity against Tetrahymena pyriformis: focusing on applicability domain and overfitting by variable selection. J Chem Inf Model. 2008;48(9):1733-46. DOI: 10.1021/ci800151m

[44] Jonhos NN, Leone FG. Statistic and experimental design in engineering and the physical sciences. New York: John Wiley & Sons; 1977. 1082 p.

[45] Sushko I, Novotarskyi S, Körner R, Pandey AK, Kovalishyn VV, Prokopenko VV, et al. Applicability domain for in silico models to achieve accuracy of experimental measurements. J Chemom. 2010;24:202-8. DOI: 10.1002/cem.1296

[46] OCHEM user's manual - OCHEM docs [Internet]. Ochem.eu. 2025 [cited 2024 Sept 9]. Available from: https://docs.ochem.eu/x/AwBa.html

[47] Bauer AW, Kirby WM, Sherris JC, Turck M. Antibiotic susceptibility testing by a standardized single disk method. Am J Clin Pathol. 1966;45:493-6. DOI: 10.1093/ajcp/45.4_ts.493

[48] Brown A, Kumar S, Tchounwou PB. Cisplatin-based chemotherapy of human cancers. J Cancer Sci Ther. 2019;11(4):97.

[49] da Nóbrega Alves D, Monteiro AFM, Andrade PN, Lazarini JG, Abílio GMF, Guerra FQS, et al. Docking prediction, antifungal activity, anti-biofilm effects on Candida spp., and toxicity against human cells of cinnamaldehyde. Molecules. 2020;25:5969. DOI: 10.3390/molecules25245969

[50] Li H, Kong Y, Hu W, Zhang S, Wang W, Yang M, et al. Litsea cubeba essential oil: Component analysis, anti-Candida albicans activity and mechanism based on molecular docking. J Oleo Sci. 2022;71:1221-8. DOI: 10.5650/jos.ess22108

[51] Tonthat NK, Juvvadi PR, Zhang H, Lee SC, Venters R, Spicer L, et al. Structures of pathogenic fungal FKBP12s reveal possible self-catalysis function. mBio. 2016;7:e00492-16. DOI: 10.1128/mBio.00492-16

[52] Srivastava V, Singla RK, Dubey AK. Inhibition of biofilm and virulence factors of *Candida albicans* by partially purified secondary metabolites of *Streptomyces chrestomyceticus* strain ADP4. Curr Top Med Chem. 2018;18:925-45. DOI: 10.2174/1568026618666180711154110

[53] Flamandita D, Sahlan M, Lischer K, Pratami DK. Molecular Docking analysis of anti-Candida albicans biomarkers in Sulawesi propolis against secreted aspartic proteinase-5. In: Proceedings of 2019 IEEE 6th International Conference on Engineering Technologies and Applied Sciences; 2019; Kuala Lumpur, Malaysia. DOI: 10.1109/ICETAS48360.2019.9117300

[54] Sinha K, Rule GS. The structure of thymidylate kinase from *Candida albicans* reveals a unique structural element. Biochemistry. 2017;56:4360-70. DOI: 10.1021/acs.biochem.7b00498

[55] Berman HM, Westbrook J, Feng Z, Gilliland G, Bhat TN, Weissig H, et al. Nucleic acids research. The Protein Data Bank. 2000; 28:235-42. DOI: 10.1093/nar/28.1.235

[56] Marvin n. n. n. (5.2.4.), 201n (2009) [Internet]. chemaxon.com [cited 2024 Sept 9]. Available from: http://www.chemaxon.com

[57] Hanwell MD, Curtis DE, Lonie DC. Avogadro: an advanced semantic chemical editor, visualization, and analysis platform. J Cheminform. 2012;4(1):4-17. DOI: 10.1186/1758-2946-4-17

[58] Alonso H, Bliznyuk AA, Gready JE. Combining docking and molecular dynamic simulations in drug design. Med Res Rev. 2006;26:531-68. DOI: 10.1002/med.20067

[59] Trott O, Olson AJ. AutoDock Vina: improving the speed and accuracy of docking with a new scoring function, efficient optimization and multithreading. J Comput Chem. 2010;31(2):455-61. DOI: 10.1002/jcc.21334

[60] Trush MM, Kovalishyn V, Ocheretniuk AD, Kobzar OL, Kachaeva MV, Brovarets VS, et al. QSAR study of some 1,3-oxazolylphosphonium derivatives as new potent anti-Candida agents and their toxicity evaluation. Curr Drug Discov Technol. 2019;16(2):204-9. DOI: 10.2174/1570163815666180418145422

[61] Hodyna D, Kovalishyn V, Semenyuta I, Rogalsky S, Gryniukova A, Metelytsia L. Ester-functionalized imidazolium-and pyridinium-based ionic liquids: design, synthesis and cytotoxicity evaluation. Biointerface Res Appl Chem. 2022;12(3):2905-57. DOI: 10.33263/BRIAC123.29052957

[62] Monk BC, Sagatova AA, Hosseini P, Ruma YN, Wilson RK, Keniya MV. Fungal Lanosterol 14α-demethylase: A target for next-generation antifungal design. Biochim Biophys Acta Proteins Proteom. 2020;1868(3):140206. DOI: 10.1016/j.bbapap.2019.02.008

[63] Aimanianda V, Simenel C, Garnaud C, Clavaud C, Tada R, Barbin L, et al. The dual activity responsible for the elongation and branching of β-(1,3)-glucan in the fungal cell wall. mBio. 2017;8:e00619-17. DOI: 10.1128/mBio.00619-17

[64] Jayasheela K, Al-Wahaibi LH, Periandy S, Hassan HM, Sebastian S, Xavier S, et al. Probing vibrational activities, electronic properties, molecular docking and Hirshfeld surfaces analysis of 4-chlorophenyl ({[(1E)-3-(1H-imidazol-1-yl)-1-phenylpropylidene] amino} oxy) methanone: A promising anti-Candida agent. J Mol Struct. 2018;1159:83-95. DOI: 10.1016/j.molstruc.2018.01.042

[65] Li W, Yu D, Gao S, Lin J, Chen Z, Zhao W. Role of Candida albicans-secreted aspartyl proteinases (Saps) in severe early childhood caries. Int J Mol Sci. 2014;15(6):10766-79. DOI: 10.3390/ijms150610766

[66] Sun S, Yang Q, Sheng Y, Fu Y, Sun C, Deng C. Investigational drugs with dual activity against HBV and HIV (Review). Exp Ther Med. 2021;21(1):35. DOI: 10.3892/etm.2020.9467

[67] Sun M, Qin J, Kang Y, Zhang Y, Ba M, Yang H, et al. 2-Methoxydiol derivatives as new tubulin and HDAC dual-targeting inhibitors, displaying antitumor and antiangiogenic response. Bioorg Chem. 2022;120:105625. DOI: 10.1016/j.bioorg.2022.105625

[68] Balbuena-Rebolledo I, Rivera-Antonio AM, Sixto-López Y, Correa-Basurto J, Rosales-Hernández MC, Mendieta-Wejebe JE, et al. Dihydropyrazole-carbohydrazide derivatives with dual activity as antioxidant and anti-proliferative drugs on breast cancer targeting the HDAC6. Pharmaceuticals. 2022;15(6):690. DOI: 10.3390/ph15060690

[69] Shaker AMM, Abdelall EKA, Abdellatif KRA, Abdel-Rahman HM. Synthesis and biological evaluation of 2-(4-methylsulfonyl phenyl) indole derivatives: multi-target compounds with dual antimicrobial and anti-inflammatory activities. BMC Chem. 2020;14:23. DOI:10.1186/s13065-020-00675-5

[70] Jachak GR, Ramesh R, Sant DG, Jorwekar SU, Jadhav MR, Tupe SG, et al. Silicone incorporated morpholine antifungals: design, synthesis, and biological evaluation. ACS Med. Chem. Lett. 2015;6:1111-6. DOI: 10.1021/acsmedchemlett.5b00245

[71] Rani N, Sharma A, Gupta GK, Singh R. Imidazoles as potential antifungal agents: a review. Mini Rev Med Chem. 2013;13:1626-55. DOI: 10.2174/13895575113139990069

[72] Schrekker HS, Donato RK, Fuentefria AM, Bergamo V, Oliveira LF, Machado MM. Imidazolium salts as antifungal agents: activity against emerging yeast pathogens, without human leucocyte toxicity. Med Chem Commun. 2013;4:1457-60. DOI: 10.1039/C3MD00222E

[73] Bergamo VZ, Donato RK, Dalla Lana DF, Donato KJZ, Ortega GG, Schrekker HS, et al. Imidazolium salts as antifungal agents: strong antibiofilm activity against multidrug-resistant Candida tropicalis isolates. Lett Appl Microbiol. 2014;60:66-71. DOI: 10.1111/lam.12338

[74] Kiran Kumar Reddy G, Nancharaiah YV. Alkylimidazolium ionic liquids as antifungal alternatives: antibiofilm activity against *Candida albicans* and underlying mechanism of action. Front Microbiol. 2020;11:730. DOI: 10.3389/fmicb.2020.00730

[75] Przestalski S, Sarapuk J, Kleszczyńska H, Gabrielska J, Hładyszowski J, Trela Z, et al. Influence of amphiphilic compounds on membranes. Acta Biochim Pol. 2000;47:627-38.

Д. Година[1], В. Ковалішин[1], Ю. Шульга[1], О. Трохименко[2], О. Аксеновська[1], С. Рогальський[1], Л. Метелиця[1]

[1]Інститут біоорганічної хімії та нафтохімії ім. В.П. Кухаря Національної академії наук України, Київ, Україна
[2]Національний університет охорони здоров'я України імені П.Л. Шупика, Київ, Україна

ПРОТИГРИБКОВА АКТИВНІСТЬ І ЦИТОТОКСИЧНІСТЬ ЛІЗОСОМОТРОПНИХ ДЕТЕРГЕНТІВ НА ОСНОВІ ПОХІДНИХ ІМІДАЗОЛУ ТА МОРФОЛІНУ

Проблематика. Поширення інфекційних захворювань, викликаних лікарсько-стійкими бактеріальними та грибковими штамами, особливо нозокоміальними, є серйозною проблемою сучасної медицини. Відомо, що гриб *Candida albicans* є найпоширенішим збудником кандидозної інфекції, в т.ч. важкої форми. Виникнення та швидке формування лікарської резистентності як фактора ризику при лікуванні онкологічних захворювань, обтяжених кандидозною інфекцією, потребує нових терапевтичних підходів, зокрема вивчення синтетичних біорегуляторів із протигрибковою та протипухлинною ефективністю.
Мета. Синтез і дослідження протигрибкової активності та цитотоксичності лізосомотропних детергентів (ЛД) на основі похідних імідазолу та морфоліну, що містять як додецильні радикали, так і складноефірні функціональні довгі алкільні ланцюги.
Методика реалізації. Для розробки QSAR-моделей за допомогою платформи OCHEM було використано методи машинного навчання Transformer Convolutional Neural Network (Trans-CNN), Transformer Convolutional Neural Fingerprint (Trans-CNF) та Random Forest (RF). Лізосомотропні детергенти на основі похідних імідазолу та морфоліну, що містять як додецильні радикали, так і складноефірні функціональні довгі алкільні ланцюги, були синтезовані й охарактеризовані за допомогою спектроскопії ядерного магнітного резонансу. Протигрибкові властивості досліджених сполук визначали диско-дифузійним методом щодо *C. albicans* ATCC 10231 і клінічних ізолятів *C. albicans*, *C. glabrata* та *C. krusei*. Цитотоксичну дію ЛД оцінювали *in vitro* за показ-

ником IC_{50} проти лінії ракових клітин гортані людини HEp-2. Програмне забезпечення AutoDock Vina було використано для оцінки синтезованих сполук як лігандів кількох протигрибкових мішеней.
Результати. Ідентифіковані та синтезовані ЛД на основі похідних імідазолу та морфоліну виявили високий протигрибковий потенціал проти всіх видів *Candida*, зокрема проти стійких до флуконазолу клінічних ізолятів *C. albicans*, *C. glabrata* та *C. krusei*. Встановлено, що ЛД 1 (IM-C_{12}) на основі імідазолу та ЛД 4 (Mor-C_{12}) на основі морфоліну виявилися найбільш активними щодо досліджуваних штамів грибів. Результати молекулярного докінгу свідчать, що протигрибкові механізми сполук можуть бути пов'язані з інгібуванням грибкової ланостерол 14α-деметилази. Результати цитотоксичних досліджень синтезованих сполук проти лінії ракових клітин HEp-2 продемонстрували, що ЛД на основі похідних морфоліну менш цитотоксичні порівняно з ЛД на основі похідних імідазолу.
Висновки. Встановлено, що ЛД IM-C_{12} (1) є найбільш перспективним цитостатиком і протигрибковим засобом. ЛД IM-CH_2COOC_{10} (2) і Mor-C_{12} (4) за умов хімічної модифікації, в т.ч. вуглеводневого ланцюга, також можуть бути цікаві в напрямі розробки потенційних протиракових засобів.
Ключові слова: лізосомотропні детергенти; 1-алкілімідазол; N-алкілморфолін; антикандидозна активність; цитотоксичність; молекулярний докінг; QSAR.

Supplementary materials

1. Results and discussion

1.1 Parameters of the Regression models

Table S1: Statistical coefficients of the regression models

N	Method	Training Set[a]			Test Set[a]		
		R^2	q^2	RMSE[c]	R^2	q^2	RMSE
1	Trans-CNN	0.72 ± 0.02	0.72 ± 0.02	0.49 ± 0.01	0.73 ± 0.03	0.73 ± 0.03	0.48 ± 0.02
2	Trans-CNF	0.72 ± 0.02	0.72 ± 0.02	0.5 ± 0.02	0.72 ± 0.04	0.72 ± 0.04	0.49 ± 0.03
3	RF	0.73 ± 0.02	0.72 ± 0.02	0.5 ± 0.01	0.72 ± 0.03	0.71 ± 0.03	0.49 ± 0.03
4	Consensus[b]	0.75 ± 0.01	0.75 ± 0.01	0.47 ± 0.01	0.74 ± 0.03	0.74 ± 0.03	0.47 ± 0.03

[a]The training and test datasets comprised 1073 and 268 molecules, respectively. [b]The consensus model was created by taking a simple average of the Trans-CNN, RF, and Trans-CNF models. [c]RMSE stands for root mean square error, while R^2 and q^2 represent the squared linear correlation and coefficient of determination, respectively.

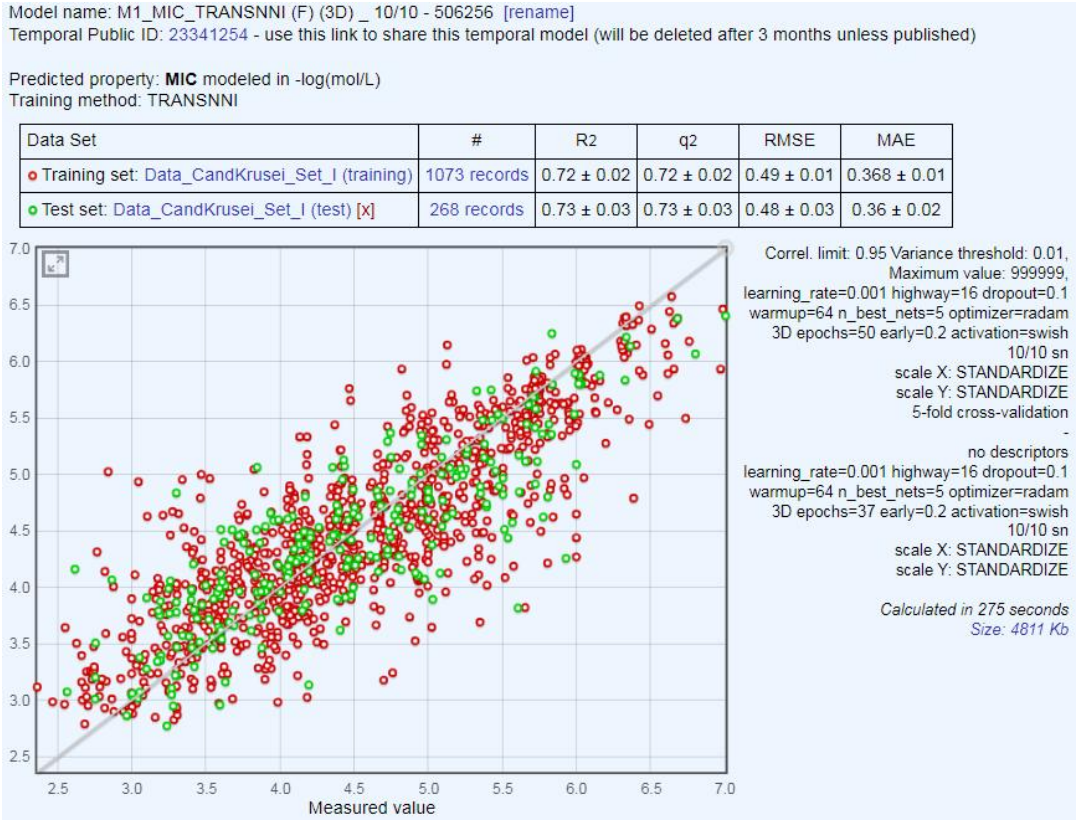

a

Model name: M2_MIC_CNF2 (F) (3D) _ 25/25 - 506261 [rename]
Temporal Public ID: 32656674 - use this link to share this temporal model (will be deleted after 3 months unless published)

Predicted property: **MIC** modeled in -log(M)
Training method: CNF2

Data Set	#	R2	q2	RMSE	MAE
Training set: Data_CandKrusei_Set_I (training)	1073 records	0.72 ± 0.02	0.72 ± 0.02	0.5 ± 0.01	0.36 ± 0.01
Test set: Data_CandKrusei_Set_I (test) [x]	268 records	0.72 ± 0.04	0.72 ± 0.04	0.49 ± 0.03	0.36 ± 0.02

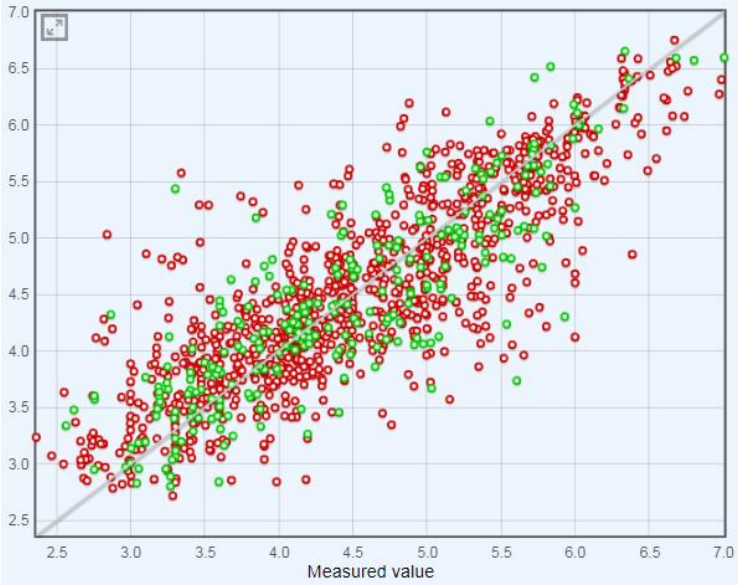

Correl. limit: 0.95 Variance threshold: 0.01,
Maximum value: 999999,
mlp=64 n_filters=19 learning_rate=0.001
highway=16 dropout=0.1 warmup=64
n_best_nets=5 optimizer=radam 3D
epochs=50 early=0.2 activation=swish 25/25
scale X: STANDARDIZE
scale Y: STANDARDIZE
5-fold cross-validation
-
no descriptors
mlp=64 n_filters=19 learning_rate=0.001
highway=16 dropout=0.1 warmup=64
n_best_nets=5 optimizer=radam 3D
epochs=23 early=0.2 activation=swish 25/25
scale X: STANDARDIZE
scale Y: STANDARDIZE

Calculated in 1865 seconds
Size: 5327 Kb

b

Model name: M3_MIC_RFR _[ALogPS, CDK23 (cons,topol,geom,elect,hybr), OEstate] - 506137 [rename]
Temporal Public ID: 50930587 - use this link to share this temporal model (will be deleted after 3 months unless published)

Predicted property: **MIC** modeled in -log(M)
Training method: RFR

Data Set	#	R2	q2	RMSE	MAE
Training set: Data_CandKrusei_Set_I (training)	1017 records	0.73 ± 0.02	0.72 ± 0.01	0.5 ± 0.01	0.38 ± 0.01
Test set: Data_CandKrusei_Set_I (test) [x]	250 records	0.72 ± 0.03	0.71 ± 0.03	0.49 ± 0.03	0.36 ± 0.02

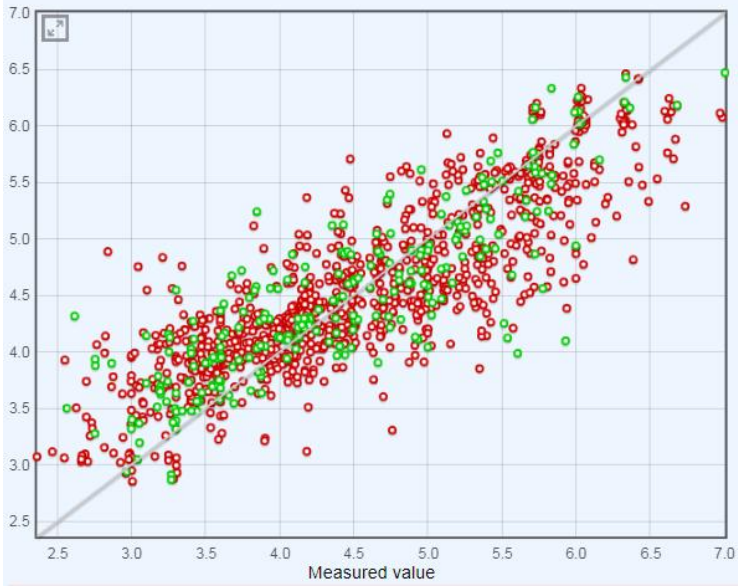

[ALogPS, CDK23
(cons,topol,geom,elect,hybr), OEstate]
Correl. limit: 0.95 Variance threshold: 0.01,
Maximum value: 999999,
trees=512 3D by RDKIT3D
5-fold cross-validation
-
339 pre-filtered descriptors
trees=512

Calculated in 1863 seconds
Size: 3782 Kb

c

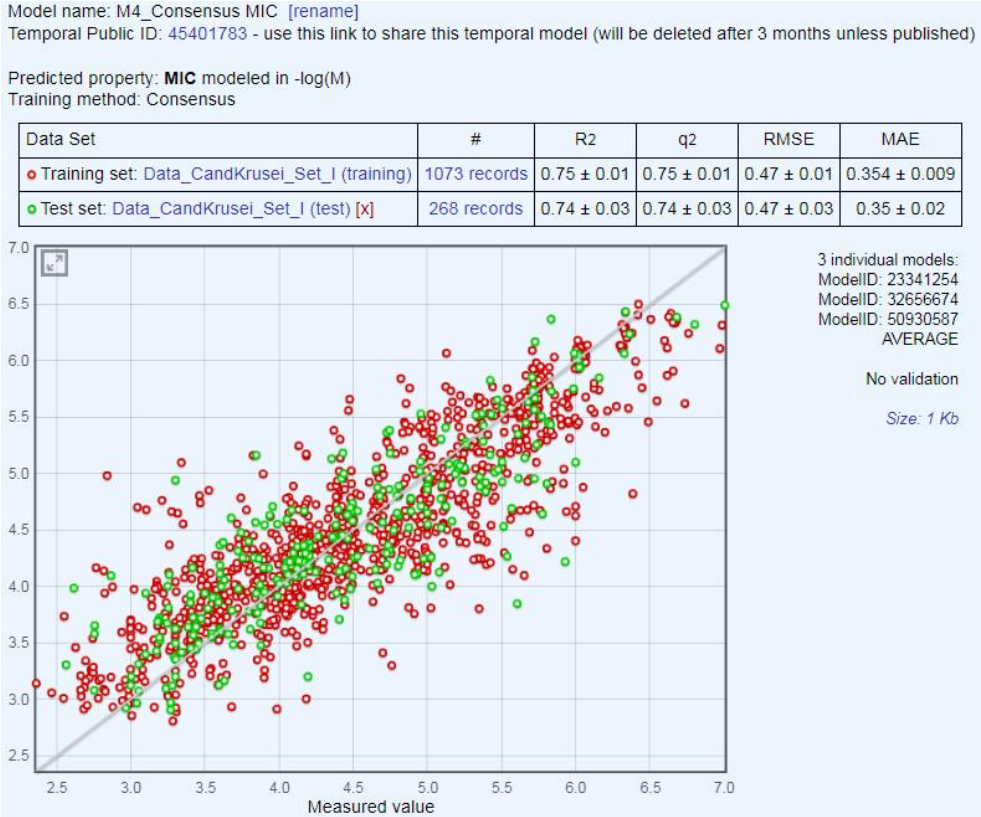

d

Figure S1: QSAR models developed using the OCHEM (http://ochem.eu): (a)–(c) statistical coefficients calculated for regression models by a different MLT; (d) consensus model calculated by averaging the previous three models

The previously published classification models [i] were created by the *Associative Neural Networks* (ASNN) [ii] and WEKA-RF methods [iii] using the On-line Chemical Database and Modeling Environment. (https://ochem.eu/article/105760) (see Fig. S2).

Model name: Antifungal activity_ASNN[EState, ALogPS, Dragon7 (blocks: 1-30)], 268016 [rename] , published in QSAR oxazolylphosphonium derivatives as new potent anti-Candida agents and their toxicity evaluation.
Public ID is 698

Predicted property: **Antifungal activity** modeled in CLASS
Training method: ASNN

Data Set	#	Accuracy	Balanced Accuracy	MCC	AUC
Training set: Candida_Albicans (training)	688 records	91% ± 1.0	91% ± 1.0	0.82 ± 0.02	0.96 ± 0.008
Test set: Candida_Albicans (test) [x]	231 records	91% ± 2.0	91% ± 2.0	0.82 ± 0.04	0.97 ± 0.01

Show ROC curves

Real↓/Predicted→	active	inactive	Hit rate
active	339	36	0.9
inactive	27	286	0.91
Precision	0.93	0.89	

Training (Original)

Real↓/Predicted→	active	inactive	Hit rate
active	119	10	0.92
inactive	11	91	0.89
Precision	0.92	0.9	

Test (Original)

a

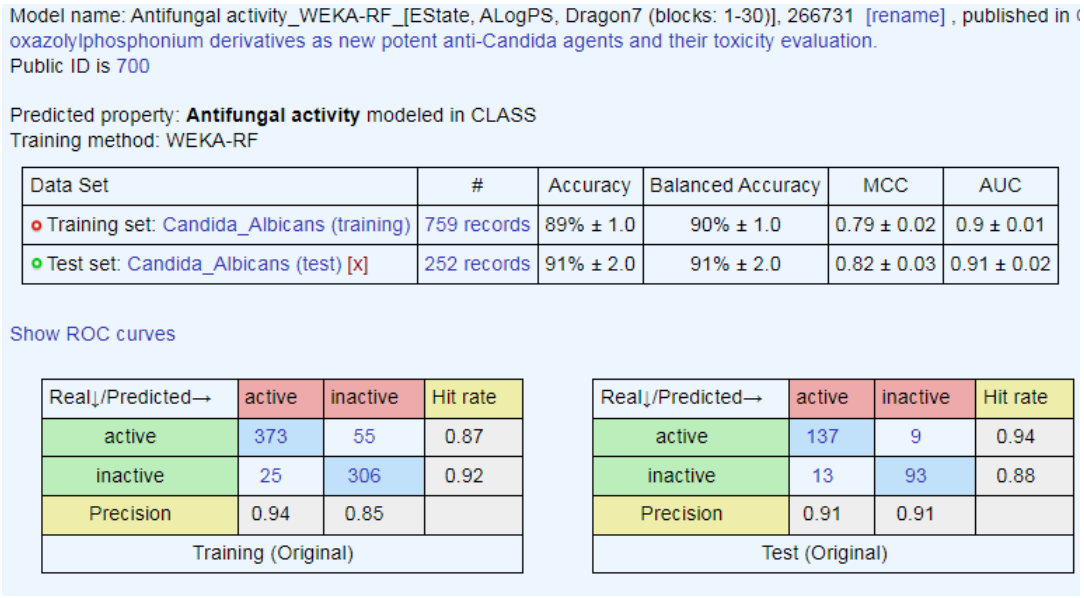

Model name: Antifungal activity_WEKA-RF_[EState, ALogPS, Dragon7 (blocks: 1-30)], 266731 [rename] , published in (oxazolylphosphonium derivatives as new potent anti-Candida agents and their toxicity evaluation.
Public ID is 700

Predicted property: **Antifungal activity** modeled in CLASS
Training method: WEKA-RF

Data Set	#	Accuracy	Balanced Accuracy	MCC	AUC
Training set: Candida_Albicans (training)	759 records	89% ± 1.0	90% ± 1.0	0.79 ± 0.02	0.9 ± 0.01
Test set: Candida_Albicans (test) [x]	252 records	91% ± 2.0	91% ± 2.0	0.82 ± 0.03	0.91 ± 0.02

Show ROC curves

Real↓/Predicted→	active	inactive	Hit rate
active	373	55	0.87
inactive	25	306	0.92
Precision	0.94	0.85	
Training (Original)			

Real↓/Predicted→	active	inactive	Hit rate
active	137	9	0.94
inactive	13	93	0.88
Precision	0.91	0.91	
Test (Original)			

b

Figure S2: Classification machine learning models built by the OCHEM server [iv]: (a) statistical coefficients calculated for classification models by ASNN; (b) statistical coefficients calculated for classification models by WEKA-RF. The training and test sets included 763 and 254 molecules, respectively

1.2 Prediction of compound activity by regression models

Table S2: Structures of the 6 compounds analyzed in this work

Comp. No	Chemical Structure	Weight	Chemical Name
1	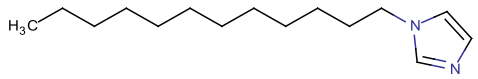	236.4	1-Dodecylimidazole
2	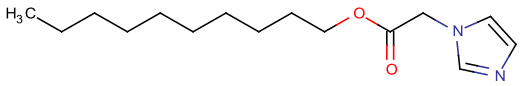	266.4	1-Decyloxycarbonylmethylimidazole
3	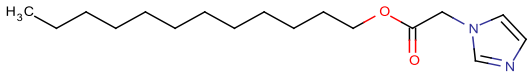	294.4	1-Dodecyloxycarbonylmethylimidazole
4	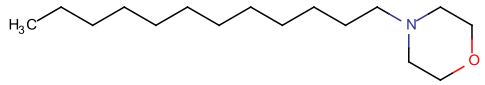	255.4	N-dodecylmorpholine
5	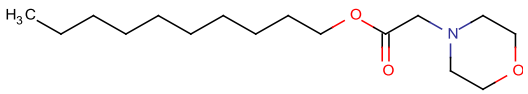	285.4	N-decyloxycarbonylmethylmorpholine
6	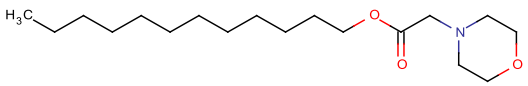	313.5	N-dodecyloxycarbonylmethylmorpholine

References

[i]. Trush MM, Kovalishyn V, Ocheretniuk AD, Kobzar OL, Kachaeva MV, Brovarets VS, & Metelytsia LO. QSAR study of some 1,3-oxazolylphosphonium derivatives as new potent anti-Candida agents and their toxicity evaluation. Curr Drug Discov Technol. 2019;16(2):204-9. DOI: 10.2174/1570163815666180418145422

[ii]. Tetko IV. Associative neural network. Methods Mol Biol. 2008;458:185-202. DOI: 10.1007/978-1-60327-101-1_10

[iii]. Livingston F. Implementation of Breiman's random forest machine learning algorithm. ECE591Q Mach Learn J Pap. 2005;1:1-13.